

Light-Shifts of an Integrated Filter-Cell Rubidium Atomic Clock

May 25, 2015

James C. Camparo
Electronics and Photonics Laboratory
Physical Sciences Laboratories

Prepared for:

Space and Missile Systems Center
Air Force Space Command
483 N. Aviation Blvd.
El Segundo, CA 90245-2808

Contract No. FA8802-14-C-0001

Authorized by: Engineering and Technology Group

Distribution Statement A: Approved for public release; distribution unlimited.

Report Documentation Page

Form Approved
OMB No. 0704-0188

Public reporting burden for the collection of information is estimated to average 1 hour per response, including the time for reviewing instructions, searching existing data sources, gathering and maintaining the data needed, and completing and reviewing the collection of information. Send comments regarding this burden estimate or any other aspect of this collection of information, including suggestions for reducing this burden, to Washington Headquarters Services, Directorate for Information Operations and Reports, 1215 Jefferson Davis Highway, Suite 1204, Arlington VA 22202-4302. Respondents should be aware that notwithstanding any other provision of law, no person shall be subject to a penalty for failing to comply with a collection of information if it does not display a currently valid OMB control number.

1. REPORT DATE 25 MAY 2015	2. REPORT TYPE Final	3. DATES COVERED -			
4. TITLE AND SUBTITLE Light-Shifts of an Integrated Filter-Cell Rubidium Atomic Clock		5a. CONTRACT NUMBER FA8802-14-C-0001			
		5b. GRANT NUMBER			
		5c. PROGRAM ELEMENT NUMBER			
6. AUTHOR(S) James C. Camparo		5d. PROJECT NUMBER			
		5e. TASK NUMBER			
		5f. WORK UNIT NUMBER			
7. PERFORMING ORGANIZATION NAME(S) AND ADDRESS(ES) The aerospace Corporation 2310 E. El Segundo Blvd. El Segundo, CA 90245-4609		8. PERFORMING ORGANIZATION REPORT NUMBER TOR-2015-02236			
9. SPONSORING/MONITORING AGENCY NAME(S) AND ADDRESS(ES) Space and Missile Systems Center Air Force Space Command 483 N. Aviation Blvd. El Segundo, CA 90245-2808		10. SPONSOR/MONITOR'S ACRONYM(S) SMC			
		11. SPONSOR/MONITOR'S REPORT NUMBER(S)			
12. DISTRIBUTION/AVAILABILITY STATEMENT Approved for public release, distribution unlimited					
13. SUPPLEMENTARY NOTES The original document contains color images.					
14. ABSTRACT					
15. SUBJECT TERMS					
16. SECURITY CLASSIFICATION OF:			17. LIMITATION OF ABSTRACT UU	18. NUMBER OF PAGES 11	19a. NAME OF RESPONSIBLE PERSON
a. REPORT unclassified	b. ABSTRACT unclassified	c. THIS PAGE unclassified			

PHYSICAL SCIENCES LABORATORIES

The Aerospace Corporation functions as an “architect-engineer” for national security programs, specializing in advanced military space systems. The Corporation's Physical Sciences Laboratories support the effective and timely development and operation of national security systems through scientific research and the application of advanced technology. Vital to the success of the Corporation is the technical staff's wide-ranging expertise and its ability to stay abreast of new technological developments and program support issues associated with rapidly evolving space systems. Contributing capabilities are provided by these individual organizations:

Electronics and Photonics Laboratory: Microelectronics, VLSI reliability, failure analysis, solid-state device physics, compound semiconductors, radiation effects, infrared and CCD detector devices, data storage and display technologies; lasers and electro-optics, solid-state laser design, micro-optics, optical communications, and fiber-optic sensors; atomic frequency standards, applied laser spectroscopy, laser chemistry, atmospheric propagation and beam control, LIDAR/LADAR remote sensing; solar cell and array testing and evaluation, battery electrochemistry, battery testing and evaluation.

Space Materials Laboratory: Evaluation and characterizations of new materials and processing techniques: metals, alloys, ceramics, polymers, thin films, and composites; development of advanced deposition processes; nondestructive evaluation, component failure analysis and reliability; structural mechanics, fracture mechanics, and stress corrosion; analysis and evaluation of materials at cryogenic and elevated temperatures; launch vehicle fluid mechanics, heat transfer and flight dynamics; aerothermodynamics; chemical and electric propulsion; environmental chemistry; combustion processes; space environment effects on materials, hardening and vulnerability assessment; contamination, thermal and structural control; lubrication and surface phenomena. Microelectromechanical systems (MEMS) for space applications; laser micromachining; laser-surface physical and chemical interactions; micropropulsion; micro- and nanosatellite mission analysis; intelligent microinstruments for monitoring space and launch system environments.

Space Science Applications Laboratory: Magnetospheric, auroral and cosmic-ray physics, wave-particle interactions, magnetospheric plasma waves; atmospheric and ionospheric physics, density and composition of the upper atmosphere, remote sensing using atmospheric radiation; solar physics, infrared astronomy, infrared signature analysis; infrared surveillance, imaging and remote sensing; multispectral and hyperspectral sensor development; data analysis and algorithm development; applications of multispectral and hyperspectral imagery to defense, civil space, commercial, and environmental missions; effects of solar activity, magnetic storms and nuclear explosions on the Earth's atmosphere, ionosphere and magnetosphere; effects of electromagnetic and particulate radiations on space systems; space instrumentation, design, fabrication and test; environmental chemistry, trace detection; atmospheric chemical reactions, atmospheric optics, light scattering, state-specific chemical reactions, and radiative signatures of missile plumes.

Light-Shifts of an Integrated Filter-Cell Rubidium Atomic Clock

James Camparo

Physical Sciences Laboratories

The Aerospace Corporation, PO Box 92957, Los Angeles, CA 90009

Abstract

In this work, we consider the light-shift coefficients observed in rubidium (Rb) atomic frequency standards, and how the units of measurement reported for light-shift coefficients trace back to the underlying physical parameters of the light-shift. We then measure the light-shift coefficient in an integrated filter-cell, commercial Rb clock, which is similar to the Rb clock design currently flying on Galileo and BeiDou satellites. We measure the light-shift coefficient for two different rf-discharge lamps (i.e., a pure ^{87}Rb lamp and a lamp filled with the natural Rb isotope abundance), and show that under certain conditions it is possible to combine light-shift data. Our light-shift coefficients are consistent with those reported for the Galileo Rb clock under the assumption of a natural (or ^{85}Rb isotopically enriched) rf-discharge lamp for the Galileo clock.

I. Introduction

Overview

The rubidium (Rb) atomic frequency standard is the workhorse of precise atomic timekeeping in space due to its low weight, small volume, and low power consumption [1]. Moreover, the device has excellent frequency stability out to (and beyond) 10^4 seconds averaging time, rivaling the performance of passive hydrogen masers [2,3]. However, one of the clock's more significant issues is long-term frequency drift, which may be related to the light-shift effect [4,5]: a basic physics atomic perturbation that causes the Rb clock's output frequency to depend on the intensity of (atomic-signal-producing) lamplight. Moreover, on-orbit Rb atomic clocks have displayed frequency jumps that are correlated with lamplight jumps [6,7]. Thus, understanding the light-shift effect has both basic and applied physics implications.

Here we discuss our measurements of the light shift effect in a commercial, *integrated filter-cell* [8], Rb atomic clock, similar to the Rb atomic clock flying on Galileo GNSS satellites [9]. As illustrated in Fig. 1, the physics package of the prototypical Rb clock (i.e., the *separated filter-cell* clock) is composed of a lamp, a filter cell, a resonance cell, and a photodetector, with the resonance cell inside a microwave cavity that is tuned to the ^{87}Rb atom's hyperfine resonance frequency of 6834.7 MHz. The lamplight passes through the filter cell, and in so doing has its optical spectrum "shaped" so that it can efficiently produce an atomic signal via the process known as optical pumping [10,11]. As a consequence of optical pumping, the steady-state population of atoms in the absorbing hyperfine level (i.e., $F=1$) is reduced, and so the Rb vapor in the resonance cell becomes (to some degree) transparent to the lamplight. With the Rb vapor absorbing little lamplight, more light passes through to the photodiode.

If microwaves are applied to the vapor at the hyperfine resonance frequency, atoms are forced by the microwave signal to return to the absorbing hyperfine state. Consequently, more lamplight gets absorbed by the vapor, and less passes through to the photodiode. The change in transmitted light corresponds to the amplitude of the atomic clock signal. The magnitude of this change will, of course, depend on the efficiency of the optical pumping process, which ultimately traces back to the filter cell's ability to optimally shape the lamplight's spectrum.

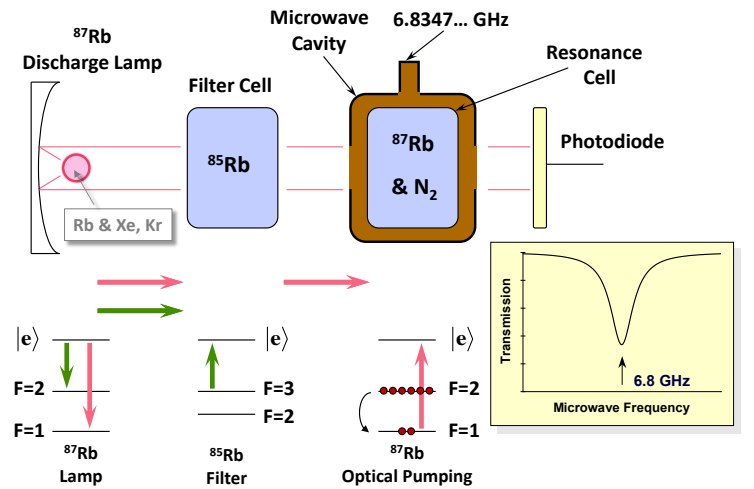


Figure 1: Block diagram of the prototypical *separated filter-cell* rubidium (Rb) atomic clock. The ^{87}Rb lamp emits spectral lines that originate in a rubidium excited state and terminate on one of the two ground-state hyperfine levels of the atom. Due to a coincidence of nature, one of these spectral lines is absorbed by the ^{85}Rb atoms in the resonance cell, allowing the other spectral line to pass through, where it can create a population imbalance between the ground-state hyperfine levels via optical pumping.

In the 1970s, Efratom, a Rb clock manufacturing company, commercialized the integrated filter-cell Rb clock [12]. For an integrated filter-cell clock, the resonance cell and filter cell are combined in one: the Rb vapor in the filter/resonance cell combination contains both rubidium isotopes. The filtering action of the lamplight by ^{85}Rb atoms occurs in the front of the filter/resonance cell, so that the ^{87}Rb atomic signal is generated towards the back of the filter/resonance cell. An advantage to the integrated filter-cell approach is that one set of heaters is eliminated from the clock's design (i.e., the separate filter-cell heater), which reduces the clock's overall power budget. We note somewhat parenthetically that the first Rb clocks flown on GPS were of an Efratom integrated filter-cell design [13], and integrated filter-cell Rb clocks have been flown on Galileo [9] and BeiDou satellites [14].

II. The Light-Shift

General Considerations

In a semiclassical formalism, the light-shift arises as a second-order interaction between an atom's induced dipole moment and the perturbing electrical field [15,16]. (For a classical description of the light shift, see the Appendix.) If we imagine the atom as a polarizable medium as illustrated in Fig. 2, with a (frequency dependent) polarizability $\alpha(\omega)$, then the perturbing electric field of the light, $\vec{E}(\omega)$, will induce a dipole moment $\vec{p}(\omega)$ in the atom:

$$\vec{p}(\omega) = \alpha(\omega)\vec{E}(\omega). \quad (1)$$

This dipole will interact with the electric field that produced it, so that to *second-order* in the electric field strength there is an interaction energy between the atom and the light, $\Delta\epsilon$:

$$\Delta\epsilon = -\frac{1}{2}\vec{p}(\omega)\cdot\vec{E}(\omega). \quad (2)$$

This interaction perturbs the atom's energy level structure, giving rise to a shift in the atom's ground-state hyperfine splitting, $h\nu_{\text{hfs}}$:

$$\frac{\delta f}{f_0} = \frac{\Delta\epsilon}{h\nu_{\text{hfs}}} = -\frac{\vec{p}(\omega)\cdot\vec{E}(\omega)}{2h\nu_{\text{hfs}}} = -\left(\frac{1}{2h\nu_{\text{hfs}}}\right)\alpha(\omega)|\vec{E}(\omega)|^2. \quad (3)$$

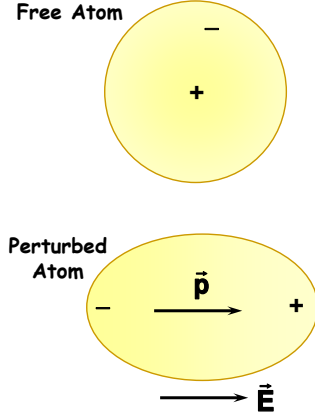


Figure 2: Illustration of an atom as a polarizable medium. In the presence of an electric field a dipole moment is induced in the atom, which can then interact with the electric field to produce a perturbation of the atom's energy level structure.

The Light-Shift Coefficient

The light-shift as expressed by Eq. (3) is valid for a monochromatic light wave. However, as is well known the lamplight's spectrum after filtering can be fairly broadband and complex [17,18], and each spectral component of the lamplight will contribute to the overall light-shift, Δy_{LS} , via Eq. (3). Consequently, if we represent the normalized intensity spectrum of the lamplight (after filtering) in the frequency range ω to $\omega+d\omega$, by $S(\omega)d\omega$:

$$\int_0^{\infty} S(\omega)d\omega = 1, \quad (4)$$

and take I_0 as the total Rb light reaching the ^{87}Rb atoms in the atomic-signal generating region of the clock's physics package, then

$$\Delta y_{\text{LS}} = I_0 \int_0^{\infty} \alpha(\omega)S(\omega)d\omega = \beta_{\text{LS}}I_0, \quad (5)$$

where β_{LS} is the light-shift coefficient of the clock. Clearly, β_{LS} will depend on the emission spectrum of the lamp as well as the filtering action in the clock.

Equation (5) is valid for the clock's full light-shift. However, we are typically not interested in the full light-shift, but rather variations in the light-shift about its average value: $\delta[\Delta y_{\text{LS}}]$, which for convenience we will write simply as δ_{LS} . Therefore, defining $\langle I_0 \rangle$ as the average light intensity emitted by the lamp we have

$$\delta_{\text{LS}} \equiv \delta[\Delta y_{\text{LS}}] = \beta_{\text{LS}}(I_0 - \langle I_0 \rangle) = \beta_{\text{LS}}\langle I_0 \rangle \frac{\Delta I}{\langle I_0 \rangle} = \kappa_{\text{LS}} \frac{\Delta I}{\langle I_0 \rangle}. \quad (6)$$

κ_{LS} is the parameter routinely reported in the literature for a clock's light-shift coefficient, typically in units of $\%^{-1}$. However, as can readily be seen from Eq. (6), clock-to-clock comparisons among κ_{LS} values should be treated with caution [19], since κ_{LS} depends on $\langle I_0 \rangle$. The parameter of real comparative value is β_{LS} .

Comparing κ_{LS} Values

While caution must be exercise in comparing κ_{LS} values among clocks and clock operating conditions, there are certain situations where comparison may be possible. Specifically, let's assume that the following conditions hold for two Rb atomic clocks: Clock #1 and Clock #2

- The filtering action of the clocks is similar. Specifically, the two clocks are both either separated filter cell or integrated filter cell. Additionally, we assume that the optical depth of the ^{85}Rb filtering vapor is similar in the two clocks.
- The rf-discharge lamps of the two clocks operate with similar electronics, so that the degrees of plasma ionization and the electron temperatures are not too dissimilar [20].
- The lamps of the two clocks have the same Rb isotope composition (*e.g.*, pure ^{87}Rb or natural Rb – 72.2% ^{85}Rb and 27.8% ^{87}Rb).
- The lamps operate at not too dissimilar temperatures.

Given these assumptions, β_{LS} for the two clocks should be the same, leaving only $\langle I_0 \rangle$ to differ. Considering Eq. (6) for the two clocks, we then have

$$\delta_{\text{LS}}(1) = \kappa_{\text{LS}}(1) \frac{\Delta I}{\langle I_0 \rangle} = \beta_{\text{LS}}\langle I_0 \rangle_2 \left(\frac{\langle I_0 \rangle_1}{\langle I_0 \rangle_2} \right) \frac{\Delta I}{\langle I_0 \rangle}, \quad (7a)$$

$$\frac{\delta_{LS}(1)}{\delta_{LS}(2)} = \frac{\kappa_{LS}(1)}{\kappa_{LS}(2)} = \left(\frac{\langle I_o \rangle_1}{\langle I_o \rangle_2} \right), \quad (7b)$$

which provides a means of comparing κ_{LS} values. (Here, we have assumed that any differences in the lamps' light intensities affects the numerator and denominator of $\Delta I/\langle I_o \rangle$ equivalently.)

We can go a bit further with this line of reasoning. Specifically, $\langle I_o \rangle$ should primarily depend on the vapor density of rubidium in the lamp [21]. Since Rb vapor density depends exponentially on the temperature of the liquid Rb pool in the lamp, all other things being equal the ratio of $\langle I_o \rangle$ for lamps #1 and #2 should be given by

$$\frac{\langle I_o \rangle_1}{\langle I_o \rangle_2} = \text{Exp} \left[\frac{\Delta G}{k_B} \left(\frac{1}{T_2} - \frac{1}{T_1} \right) \right], \quad (8)$$

where ΔG is the energy of Rb vaporization, which has the value 1.313×10^{-12} ergs [22], k_B is Boltzmann's constant, and T_J is the base temperature of lamp #J. Using Eq. (8) in Eq. (7b), we can then write

$$\frac{\delta_{LS}(1)}{\delta_{LS}(2)} = \frac{\kappa_{LS}(1)}{\kappa_{LS}(2)} = \text{Exp} \left[\frac{\Delta G}{k_B} \left(\frac{1}{T_2} - \frac{1}{T_1} \right) \right]. \quad (9)$$

III. Experiment

There are two ideas worth testing from the above: 1) κ_{LS} is strongly affected by the rf-discharge lamp's emission spectrum, and 2) δ_{LS} values are comparable (under appropriate conditions) by the simple scaling of Eq. (7b).

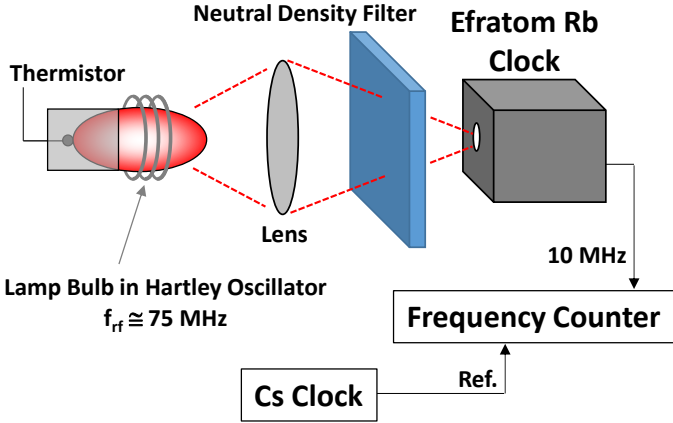


Figure 3: Light shift measurement apparatus employing a commercial, integrated filter-cell Rb atomic clock.

For our experiment, we employed a commercial FRK Rb atomic clock manufactured by Efratom [12], which has the advantage that the lamp bulb can be easily removed from the unit allowing a clear optical path from the outside to the clock's inner physics package. Using a separate external lamp for optical pumping and clock signal detection, as illustrated in Fig. 3, we placed neutral density filters in front of the lamp and recorded the Rb clock's frequency relative to a cesium (Cs) atomic clock.

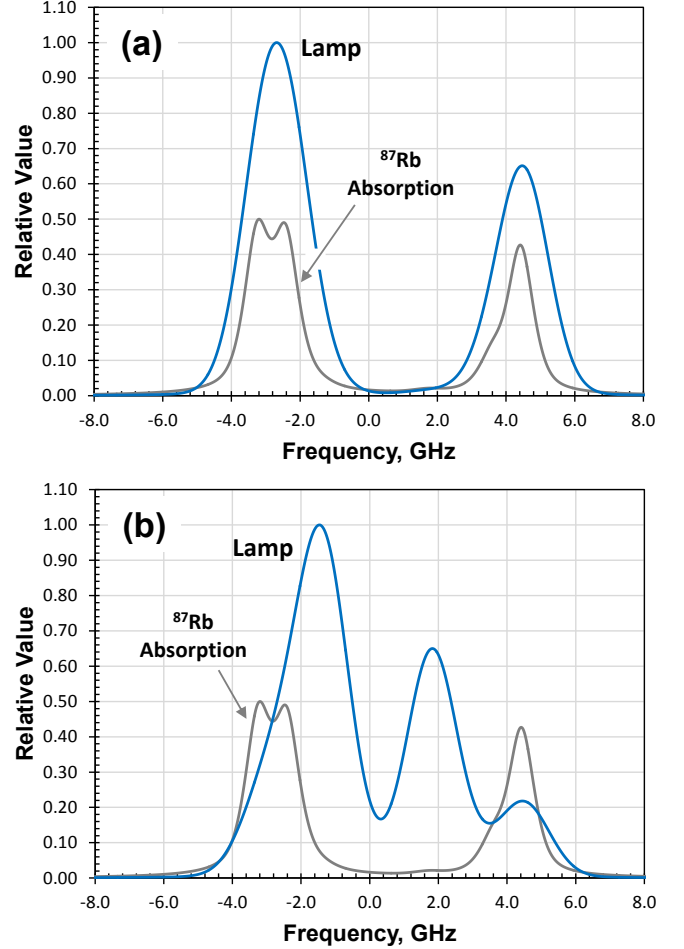


Figure 4: (a) Nominal spectrum from a pure ^{87}Rb lamp. (b) Nominal spectrum from a natural Rb lamp. For these calculated spectra we assumed a 1.6 GHz wide lamp line [23], and 40 torr of Xe as a buffer gas in the clock's resonance cell. (The actual choice of buffer gas for this figure is not particularly important.) For the pure ^{87}Rb lamp, most of the spectral intensity (*i.e.*, the lamp's "spectral weight") falls at frequencies *outside* of the ^{87}Rb hyperfine splitting; for the natural Rb lamp, most of the spectral intensity falls at frequencies *within* the hyperfine splitting.

We employed three lamps in our study, two contained pure ^{87}Rb while the third contained natural Rb. Figures 4a and 4b illustrate the different emission spectra expected for these lamps. The lamps were operated at 137 °C and 125 °C. For the lower temperature, optical elements were added to the simplified schematic shown in Fig. 3 in order to collect enough light to operate the clock. As a consequence, our results are not expected to follow Eq. (9) for the two lamp operating temperatures. However, if intensity scaling is viable for similar lamps operating under different temperatures, then our results should follow the more general Eq. (7b).

IV. Results

Figures 5a and 5b show the raw light-shift results: Fig. 5a corresponds to the natural Rb lamp, while Fig 5b shows the results for our two pure ^{87}Rb lamps. Taken in combination with

Figs. 4, these results demonstrate the dependence of κ_{LS} on lamp spectrum. Specifically, with the natural lamp's "spectral weight"* within the ^{87}Rb hyperfine splitting we expect (and find) $\kappa_{LS} > 0$; with the pure ^{87}Rb lamp's spectral weight outside of the ^{87}Rb hyperfine splitting we expect (and find) $\kappa_{LS} < 0$ [1].

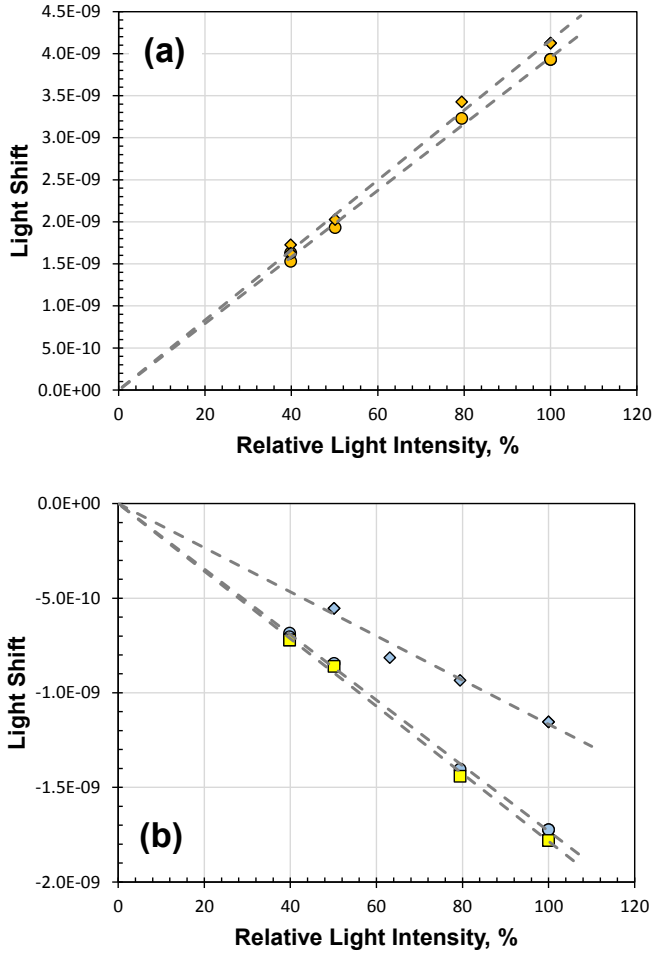


Figure 5: (a) Raw light-shift data for the natural Rb lamp: circles correspond to $T_{\text{lamp}} = 137$ °C and diamonds correspond to $T_{\text{lamp}} = 125$ °C. (b) Raw light-shift measurements for our two pure ^{87}Rb lamps: circles correspond to Lamp #1 at 137 °C; diamonds correspond to Lamp #1 at 125 °C, and squares correspond to Lamp #2 at 137 °C.

In Fig. 6, we have rescaled the raw light-shift results according to Eq. (7b). Specifically, for the natural Rb lamp we used linear regression of the raw data to compute an estimated light-shift at full light intensity for each of the temperatures. We call these estimated light-shifts $\hat{\delta}_{LS}(137)$ and $\hat{\delta}_{LS}(125)$. We then multiplied the raw light intensities for the $T_{\text{lamp}} = 125$ °C data by the ratio $\hat{\delta}_{LS}(125)/\hat{\delta}_{LS}(137)$. In effect, rather than changing the

light-shift values, we simply repositioned them along the light intensity axis. Saying this differently, we identified the 125 °C light-shifts with the normalized light intensities that they would have corresponded to for the 137 °C experiment. A similar procedure was employed for the pure ^{87}Rb lamp, except that all light intensities were repositioned based on Lamp #1's 137 °C values.

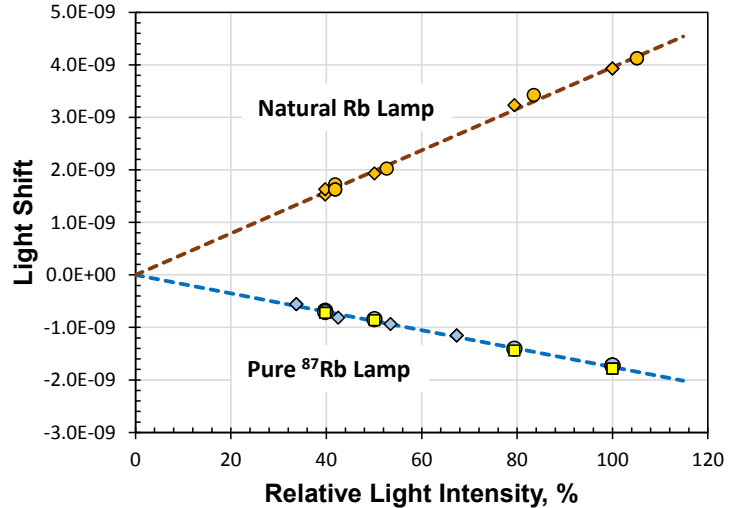


Figure 6: Rescaled light-shift measurements. Symbols are as in Fig. 5.

As Fig. 6 clearly shows, all the light-shift results for a *single type* of lamp fall on one line, which demonstrates that it is possible to rescale κ_{LS} values for similar lamps. Taken together, we find for the natural Rb lamp $\kappa_{LS} = +4.0 \times 10^{-11}/\%$, and for the pure ^{87}Rb lamp $\kappa_{LS} = -1.8 \times 10^{-11}/\%$. As noted previously, the signs of these κ_{LS} values are consistent with the lamps' spectral weights. Moreover, the relative magnitude of these κ_{LS} values is consistent with the fact that relatively more spectral intensity falls *within* the hyperfine splitting for the natural lamp than falls *outside* of the hyperfine splitting for the pure ^{87}Rb lamp.

V. Summary and Discussion

In this work, we have considered the light-shift coefficient of an integrated filter-cell Rb atomic clock operated with two different Rb rf-discharge lamps: a pure ^{87}Rb lamp and a natural Rb lamp (*i.e.*, 72.2% ^{85}Rb and 27.8% ^{87}Rb). As anticipated, the sign of the light-shift coefficient followed from a simple inspection of the spectral weight of the lamp's emission spectrum. Though the filtering action of the lamplight has the potential to significantly affect the light-shift's sign (since it is the *filtered* lamplight that ultimately determines the light-shift), in the present integrated filter-cell clock experiments the filtering was clearly not so strong as to significantly modify the effect of the lamp's spectral weight.

^{87}Rb lamp 6% more light falls outside of the hyperfine splitting than within; for the natural Rb lamp, 67% more light falls within the hyperfine splitting than outside of that splitting.

* As discussed in the caption of Fig. 4, we define the spectral weight of a lamp as the excess of intensity falling either outside the ^{87}Rb hyperfine splitting or within that splitting. Specifically, for the pure

It is interesting to note that the magnitudes of the light-shift coefficients that we obtained (even in units of %⁻¹) are not outside the range of expectation: $\sim 10^{-11}/\%$. Specifically, it has been noted that the light-shift coefficient for the separated filter-cell, Block-IIR GPS Rb clock is $-1.4 \times 10^{-12}/\%$ [7], while Droz *et al.* [24] have reported a light-shift coefficient for Galileo's integrated filter-cell clock of $+1.5 \times 10^{-10}/\%$. Additionally, Bloch *et al.* [25] provide evidence for a light-shift coefficient of $-2.2 \times 10^{-10}/\%$ for the Milstar Rb clock,[†] which is a separated filter-cell design [26]. If we assume that moving the lamp outside of the atomic clock reduces the intensity of the lamplight actually reaching the atoms in the filter/resonance cell by a factor of roughly 10, which is certainly reasonable, than our integrated filter-cell light-shift coefficients are perfectly in line with those of Droz *et al.*... assuming, of course, that the Galileo Rb atomic clock operates with a natural (or ⁸⁵Rb isotopically enriched) rf-discharge lamp.

Acknowledgement

The author would like to thank Dr. Robert Frueholz for his help in performing these experiments.

Appendix: Classical Description of the Light Shift

Though the light-shift is a consequence of an atom's quantum mechanical nature, the mechanism of the light-shift can nonetheless be understood classically [15]. As illustrated in Fig. A.1, we imagine the "classical atom" as a positive nucleus attached to a negatively charged shell with springs of force constant k [27]. Defining $x(t)$ as the deviation of a spring from its equilibrium position, the equation of motion for this atomic oscillator is just that of a damped, driven harmonic oscillator:

$$\frac{d^2x(t)}{dt^2} + 2\gamma \frac{dx(t)}{dt} + \frac{k}{m} x(t) = -\frac{e}{m} E(t). \quad (\text{A.1})$$

Here, 2γ is a damping coefficient, kx is the restoring force on the spring, m is the mass of the negative shell (*i.e.*, the electron mass) and $E(t)$ is the instantaneous value of an electric field impinging on the classical atom.

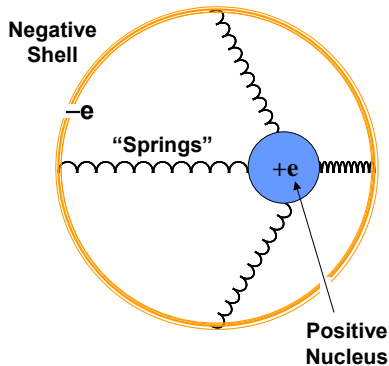


Figure A.1: The "classical atom," where the atom's negatively charged shell is attached to a positively charged nucleus via mechanical springs.

To proceed, we consider a monochromatic field such that $E(t) = E_0 \exp[i\omega t]$, where ω is the laser frequency, which allows us to write $x(t) = x_0 \exp[i\omega t]$. Using these expressions in Eq. (A.1), and defining the atom's resonant frequency, ω_0 , as $\sqrt{k/m}$ we obtain

$$x_0 = -\frac{\left(\frac{e}{m}\right)E_0}{(\omega_0^2 - \omega^2) + i2\gamma\omega}. \quad (\text{A.2})$$

Since we are only interested in optical field frequencies very near ω_0 , we can expand ω^2 in a Taylor series about ω_0 :

$$\omega^2 = \omega_0^2 + (\omega - \omega_0)2\omega_0 + (\omega - \omega_0)^2, \quad (\text{A.3})$$

and only retain the first two terms on the right-hand side of Eq. (A.3). Further, under this resonance approximation we can replace ω in the imaginary term appearing in the denominator of Eq. (2) with ω_0 , so that we finally obtain

$$x_0 = -\left(\frac{e}{2m\omega_0}\right) \frac{E_0}{((\omega_0 - \omega) + i\gamma)}. \quad (\text{A.4})$$

We now note that as the classical atom's shell oscillates relative to the location of the nucleus, an oscillating electric dipole moment will be created in the system, $p(t)$:

$$p(t) = -ex(t) = -ex_0 e^{i\omega t} = p_0 e^{i\omega t}. \quad (\text{A.5})$$

Thus, using Eq. (A.4) we obtain

$$p_0 = \left(\frac{e^2}{2m\omega_0}\right) \frac{E_0}{((\omega_0 - \omega) + i\gamma)}. \quad (\text{A.6})$$

Of course, from classical electrodynamics we know that the induced dipole moment in a dielectric medium is just given by $p(\omega) = \alpha(\omega)E(\omega)$, where $\alpha(\omega)$ is the medium's (frequency-dependent) polarizability. Using Eq. (A.6), we therefore obtain a classical expression for the polarizability of the atom:

$$\alpha(\omega) = \frac{\left(\frac{e^2}{2m\omega_0}\right)}{((\omega_0 - \omega) + i\gamma)}. \quad (\text{A.7})$$

In order to make contact with the quantum mechanical properties of the atom, Eq. (A.6) must be modified slightly in order to account for the fact that in a real atom a single energy eigenstate of the atom may be coupled with a large number of other eigenstates. We accomplish this by introducing the concept of the *oscillator strength*, f , so that Eq. (A.7) becomes [28].

[†] The light-shift coefficient was determined by examining the correlated change in clock frequency and lamplight when the vacuum system for the Rb clocks failed: See Figs. 2a and 2b in Ref. 25.

$$\alpha(\omega) = \left(\frac{e^2 f}{2m\omega_0} \right) \left(\frac{(\omega_0 - \omega) - i\gamma}{(\omega - \omega_0)^2 + \gamma^2} \right). \quad (\text{A.8})$$

As is clear from Eq. (A.8) $\alpha(\omega)$ is a complex quantity with both a real and imaginary part.

We now note that there is an interaction energy, V , between a dipole moment and an external electric field:

$$V = -\vec{p} \cdot \vec{E} = -\frac{1}{2} \alpha(\omega) |E_0|^2. \ddagger \quad (\text{A.9})$$

Given our expression for $\alpha(\omega)$, the interaction energy is also found to be complex:

$$\text{Re}[V] = \Delta\varepsilon \sim \left(\frac{e^2 f}{4m\omega_0} \right) \left(\frac{(\omega - \omega_0) I_0}{(\omega - \omega_0)^2 + \gamma^2} \right). \quad (\text{A.10a})$$

$$\text{Im}[V] \sim \left(\frac{e^2 f}{4m\omega_0} \right) \left(\frac{\gamma I_0}{(\omega - \omega_0)^2 + \gamma^2} \right). \quad (\text{A.10b})$$

The real part of the perturbation gives rise to the shift in the atom's energy levels (*i.e.*, the light shift), while the imaginary part acts like a decay term, causing transitions between energy levels. In these expressions, I_0 is the light intensity, and it is worth noting that for a monochromatic field (as considered here) if $\omega = \omega_0$ the light shift is zero.

References

1. J. Camparo, *The rubidium atomic clock and basic research*, Phys. Today, 60(11), 33-39 (2007).
2. R. T. Dupuis, T. J. Lynch, and J. R. Vaccaro, *Rubidium frequency standard for the GPS IIF program and modifications for the RAFSMOD program*, in Proc. 2008 IEEE International Frequency Control Symposium (IEEE Press, Piscataway, NJ, 2008) pp. 655-660.
3. F. Droz, P. Mosset, G. Barmaverain, P. Rochat, Q. Wang, M. Belloni, L. Mattioni, U. Schmidt, T. Pike, F. Emma, P. Waller, and G. Gatti, *Galileo rubidium standard and passive hydrogen maser – Current status and new development in Satellite Communications and Navigation Systems*, ed. E. Del Re & M. Ruggieri (Springer Science+Business Media, New York, NY, 2008) pp. 133-139.
4. J. Camparo, *A partial analysis of drift in the rubidium gas cell atomic frequency standard*, in Proc. 18th Annual Precise Time and Time Interval (PTTI) Applications and Planning Meeting, Washington, 1986 (United States Naval Observatory, Washington D. C., 1986) pp. 565-586.
5. J. Camparo, J. Hagerman, and T. McClelland, *Long-term behavior of rubidium clocks in space*, in Proc. 2012 European Frequency and Time Forum, 23-27 April, Gothenburg, Sweden, pp. 501-508.
6. J. Camparo, *Does the light shift drive frequency aging in the rubidium atomic clock?*, IEEE Ultrason., Ferroelec. and Freq. Control 52(7), 1075-1078 (2005).
7. J. Camparo, C. Klimcak, and S. Herbulock, *Frequency equilibration in the vapor-cell atomic clock*, IEEE Trans. Instrum. and Meas. 54(5), 1873-1880 (2005).
8. J. Vanier, R. Kunski, A. Brisson, and P. Paulin, *Progress and prospects in rubidium frequency standards*, J. Physique 42, Colloque C8, Supplement 12, C8-139 – C8-150 (1981).
9. H. Schweda, G. Busca, P. Rochat, *Atomic frequency standard*, United States Patent #5,387,881, 7 February 1995.
10. A. L. Bloom, *Optical pumping*, Sci. Am. 203, 72-80 (1960).
11. T. R. Carver, *Optical pumping*, Science 141(3581), 599-608 (1963).
12. E. Jechart, *A new miniature rubidium gas cell frequency standard*, in Proc. 27th Frequency Control Symposium (IEEE Press, Piscataway, NJ, 1973) pp. 387-389.
13. F. K. Koide and D. J. Dederich, *Rubidium frequency standard test program for Navstar GPS*, in Proc. 10th Annual Precise Time and Time Interval (PTTI) Systems and Planning Meeting (US Naval Observatory, Washington, DC, 1978) pp. 379-392.
14. C. Li, T. Yang, L. Zhai, and L. Ma, *Development of new-generation space-borne rubidium clock*, in China Satellite Navigation Conference (CSNC) 2013: Lecture Notes in Electrical Engineering 245 (Springer-Verlag, Berlin, 2013) Ch. 35.
15. S. Pancharatnam, *Light shifts in semiclassical dispersion theory*, J. Opt. Soc. Am. 56(11), 1636 (1966).
16. B. S. Mathur, H. Tang, and W. Happer, *Light shifts in the alkali atoms*, Phys. Rev. 171(1), 11-19 (1968).
17. T. Tako, Y. Koga, and I. Hirano, *Absorption of Rb-D lines by Rb filter cell*, Jap. J. Appl. Phys. 14(11), 1641-1646 (1975).
18. N. Kuramochi, I. Matsuda, and H. Fukuyo, *Analysis of the effect of foreign gases in the filtering action of a ⁸⁵Rb cell*, J. Opt. Soc. Am. 68(8), 1087-1092 (1978).

[‡] The factor of 1/2 comes from averaging the interaction energy over the period of the oscillating electric field.

-
19. J. Vanier, R. Kunski, P. Paulin, M. Tetu, and N. Cyr, *On the light shift in optical pumping of rubidium 87: the techniques of "separated" and "integrated" hyperfine filtering*, Can. J. Phys. 60, 1396-1403 (1982).
20. J. Camparo, F. Wang, W. Lybarger, and Y. Chan, *A complex permeability model of rf-discharge lamps*, in Proc. 2013 Precise Time and Time Interval Systems and Applications Meeting, ION PTI 2013, Bellevue, WA, December 2-5, 2013.
21. J. G. Coffer and J. C. Camparo, *rf-power and the ring-mode to red-mode transition in an inductively coupled plasma*, J. Appl. Phys. 111, 083304 (2012).
22. T. J. Killian, *Thermionic phenomenon caused by vapors of rubidium and potassium*, Phys. Rev. 27, 578-587 (1926).
23. V. B. Gerard, *Laboratory alkali metal vapour lamps for optical pumping experiments*, J. Sci. Instrum. 39, 217-218 (1962).
24. F. Droz, P. Rochat, S. Boillat, and B. Scheidegger, *GNSS RAFS latest improvement*, to be published in Proc. 2015 Joint Conference of the IEEE International Frequency Control Symposium and European Frequency and Time Forum (IEEE Press, Piscataway, NJ, 2015).
25. M. Bloch, J. Ho, T. McClelland, M. Meirs, N. D. Bhaskar, L. Mallette, and Capt. J. Hardy, *Performance data on the Milstar rubidium and quartz frequency standards: Comparison of ground tests in a simulated space environment to results obtained on orbit*, in Proc. 1996 IEEE International Frequency Control Symposium (IEEE Press, Piscataway, NJ, 1996) pp. 1057-1065.
26. T. McClelland, I. Pascaru, and M. Meirs, *Development of a rubidium frequency standard for the Milstar satellite system*, in Proc. 41st Annual Frequency Control Symposium (IEEE Press, Piscataway, NJ, 1987) pp. 66-74.
27. S. G. Lipson and H. Lipson, *Optical Physics* (Cambridge University Press, London, 1969) Ch. 10.
28. R. C. Hilborn, *Einstein coefficients, cross sections, f values, dipole moments, and all that*, Am. J. Phys. 50(11), 982-986 (1982); R. C. Hilborn, *Erratum: "Einstein coefficients, cross sections, f values, dipole moments, and all that,"* Am. J. Phys. 51(5), 471 (1983).

Light-Shifts of an Integrated Filter-Cell Rubidium Atomic Clock

Approved Electronically by:

Randy M. Villahermosa,
PRINC DIRECTOR
RESEARCH & PROGRAM
DEVELOPMENT OFFICE
TECHNOLOGY &
LABORATORY
OPERATIONS
ENGINEERING &
TECHNOLOGY GROUP

Charles L. Gustafson, SR VP
ENG & TECH
ENGINEERING &
TECHNOLOGY GROUP

Walter F. Buell, PRINC
DIRECTOR
ELECTRONICS &
PHOTONICS LABORATORY
PHYSICAL SCIENCES
LABORATORIES
ENGINEERING &
TECHNOLOGY GROUP

External Distribution

REPORT TITLE

Light-Shifts of an Integrated Filter-Cell Rubidium Atomic Clock

REPORT NO.

TOR-2015-02236

PUBLICATION DATE

May 25, 2015

SECURITY CLASSIFICATION

UNCLASSIFIED

Don Ruffin
SMC/PIC
don.ruffin.1@us.af.mil

Library
National Institute of Science
and Technology
325 Broadway, Boulder, CO
80303

Dr. K. Senior
NRL
ken.senior@nrl.navy.mil

Dr. Patrizia Tavella
Istituto Nazionale di Ricerca
Metrologica
tavella@inrim.it

Dr. Filippo Levi
Istituto Nazionale di Ricerca
Metrologica
levi@inrim.it

Library
U. S. Naval Observatory
3450 Massachusetts Ave.,
NW, Washington, DC 20392

APPROVED BY Approved by PAS (on file) DATE _____
(AF OFFICE)